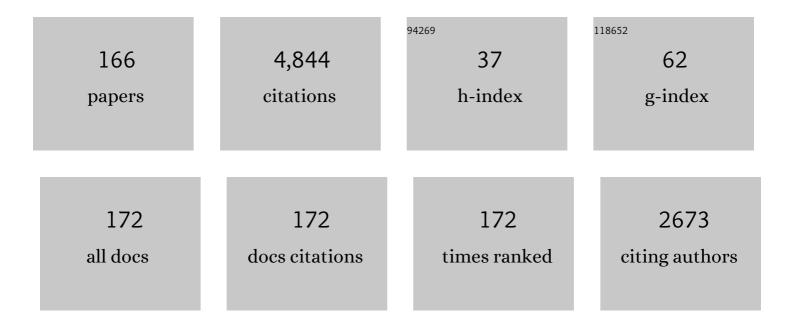
Stéphane Avril

List of Publications by Year in descending order

Source: https://exaly.com/author-pdf/5370920/publications.pdf Version: 2024-02-01



#	Article	IF	CITATIONS
1	Material Identification on Thin Shells Using the Virtual Fields Method, Demonstrated on the Human Eardrum. Journal of Biomechanical Engineering, 2022, 144, .	0.6	2
2	Stress Analysis in AAA does not Predict Rupture Location Correctly in Patients with Intraluminal Thrombus. Annals of Vascular Surgery, 2022, 79, 279-289.	0.4	5
3	A thermodynamic framework for unified continuum models for the healing of damaged soft biological tissue. Journal of the Mechanics and Physics of Solids, 2022, 158, 104662.	2.3	8
4	Atomic Force Microscopy Stiffness Mapping in Human Aortic Smooth Muscle Cells. Journal of Biomechanical Engineering, 2022, 144, .	0.6	5
5	About prestretch in homogenized constrained mixture models simulating growth and remodeling in patient-specific aortic geometries. Biomechanics and Modeling in Mechanobiology, 2022, 21, 455-469.	1.4	6
6	Computer Simulation Model May Prevent Thoracic Stent-Graft Collapse Complication. Circulation: Cardiovascular Imaging, 2022, 15, e013764.	1.3	3
7	Fluid–Structure Interaction Modeling of Ascending Thoracic Aortic Aneurysms in SimVascular. Biomechanics, 2022, 2, 189-204.	0.5	6
8	Evolving Mural Defects, Dilatation, and Biomechanical Dysfunction in Angiotensin II–Induced Thoracic Aortopathies. Arteriosclerosis, Thrombosis, and Vascular Biology, 2022, 42, 973-986.	1.1	3
9	EndoBeams.jl: A Julia finite element package for beam-to-surface contact problems in cardiovascular mechanics. Advances in Engineering Software, 2022, 171, 103173.	1.8	4
10	Sensitivity analysis of nonâ€local damage in soft biological tissues. International Journal for Numerical Methods in Biomedical Engineering, 2021, 37, e3427.	1.0	2
11	Prediction of local strength of ascending thoracic aortic aneurysms. Journal of the Mechanical Behavior of Biomedical Materials, 2021, 115, 104284.	1.5	17
12	In Vitro Measurement of Strain Localization Preceding Dissection of the Aortic Wall Subjected to Radial Tension. Experimental Mechanics, 2021, 61, 119-130.	1.1	5
13	Regulation of SMC traction forces in human aortic thoracic aneurysms. Biomechanics and Modeling in Mechanobiology, 2021, 20, 717-731.	1.4	6
14	Estimating aortic thoracic aneurysm rupture risk using tension–strain data in physiological pressure range: an in vitro study. Biomechanics and Modeling in Mechanobiology, 2021, 20, 683-699.	1.4	10
15	Design, Development, and Temporal Evaluation of a Magnetic Resonance Imaging-Compatible In Vitro Circulation Model Using a Compliant Abdominal Aortic Aneurysm Phantom. Journal of Biomechanical Engineering, 2021, 143, .	0.6	3
16	Introducing regularization into the virtual fields method (VFM) to identify nonhomogeneous elastic property distributions. Computational Mechanics, 2021, 67, 1581-1599.	2.2	11
17	Patient-specific computational evaluation of stiffness distribution in ascending thoracic aortic aneurysm. Journal of Biomechanics, 2021, 119, 110321.	0.9	8
18	Coupling hemodynamics with mechanobiology in patient-specific computational models of ascending thoracic aortic aneurysms. Computer Methods and Programs in Biomedicine, 2021, 205, 106107.	2.6	21

#	Article	IF	CITATIONS
19	General Finite-Element Framework of the Virtual Fields Method in Nonlinear Elasticity. Journal of Elasticity, 2021, 145, 265-294.	0.9	13
20	Significance of Hemodynamics Biomarkers, Tissue Biomechanics and Numerical Simulations in the Pathogenesis of Ascending Thoracic Aortic Aneurysms. Current Pharmaceutical Design, 2021, 27, 1890-1898.	0.9	1
21	Evaluation and Verification of Fast Computational Simulations of Stent-Graft Deployment in Endovascular Aneurysmal Repair. Frontiers in Medical Technology, 2021, 3, 704806.	1.3	3
22	Multi-view Digital Image Correlation Systems for In Vitro Testing of Arteries from Mice to Humans. Experimental Mechanics, 2021, 61, 1455-1472.	1.1	9
23	Material characterization of curved shells under finite deformation using the virtual fields method. Strain, 2021, 57, e12398.	1.4	2
24	Patientâ€specific computational modeling of endovascular aneurysm repair: State of the art and future directions. International Journal for Numerical Methods in Biomedical Engineering, 2021, 37, e3529.	1.0	16
25	Fiber Rearrangement and Matrix Compression in Soft Tissues: Multiscale Hypoelasticity and Application to Tendon. Frontiers in Bioengineering and Biotechnology, 2021, 9, 725047.	2.0	6
26	3D finiteâ€element modelling of vascular adaptation after endovascular aneurysm repair. International Journal for Numerical Methods in Biomedical Engineering, 2021, , e3547.	1.0	0
27	Fully-Coupled FSI Computational Analyses in the Ascending Thoracic Aorta Using Patient-Specific Conditions and Anisotropic Material Properties. Frontiers in Physiology, 2021, 12, 732561.	1.3	14
28	Relationship Between Ascending Thoracic Aortic Aneurysms Hemodynamics and Biomechanical Properties. IEEE Transactions on Biomedical Engineering, 2020, 67, 949-956.	2.5	22
29	Experimental Characterization of Adventitial Collagen Fiber Kinematics Using Second-Harmonic Generation Imaging Microscopy: Similarities and Differences Across Arteries, Species and Testing Conditions. Studies in Mechanobiology, Tissue Engineering and Biomaterials, 2020, , 123-164.	0.7	11
30	Patient Specific Computer Modelling for Automated Sizing of Fenestrated Stent Grafts. European Journal of Vascular and Endovascular Surgery, 2020, 59, 237-246.	0.8	18
31	Characterization of chemoelastic effects in arteries using digital volume correlation and optical coherence tomography. Acta Biomaterialia, 2020, 102, 127-137.	4.1	23
32	A new finiteâ€element shell model for arterial growth and remodeling after stent implantation. International Journal for Numerical Methods in Biomedical Engineering, 2020, 36, e3282.	1.0	20
33	In vitro histomechanical effects of enzymatic degradation in carotid arteries during inflation tests with pulsatile loading. Journal of the Mechanical Behavior of Biomedical Materials, 2020, 103, 103550.	1.5	4
34	Finite-Element Based Image Registration for Endovascular Aortic Aneurysm Repair. Modelling, 2020, 1, 22-38.	0.8	4
35	Deciphering ascending thoracic aortic aneurysm hemodynamics in relation to biomechanical properties. Medical Engineering and Physics, 2020, 82, 119-129.	0.8	25
36	An implicit 3D corotational formulation for frictional contact dynamics of beams against rigid surfaces using discrete signed distance fields. Computer Methods in Applied Mechanics and Engineering, 2020, 371, 113275.	3.4	7

#	Article	IF	CITATIONS
37	Hemodynamics alteration in patient-specific dilated ascending thoracic aortas with tricuspid and bicuspid aortic valves. Journal of Biomechanics, 2020, 110, 109954.	0.9	8
38	Computational Study of Growth and Remodeling in Ascending Thoracic Aortic Aneurysms Considering Variations of Smooth Muscle Cell Basal Tone. Frontiers in Bioengineering and Biotechnology, 2020, 8, 587376.	2.0	9
39	ROLE OF OXYGEN CONCENTRATION IN THE OSTEOBLASTS BEHAVIOR: A FINITE ELEMENT MODEL. Journal of Mechanics in Medicine and Biology, 2020, 20, 1950064.	0.3	8
40	Three-dimensional numerical simulation of soft-tissue wound healing using constrained-mixture anisotropic hyperelasticity and gradient-enhanced damage mechanics. Journal of the Royal Society Interface, 2020, 17, 20190708.	1.5	18
41	Multimodality Imaging-Based Characterization of Regional Material Properties in a Murine Model of Aortic Dissection. Scientific Reports, 2020, 10, 9244.	1.6	20
42	Computational prediction of hemodynamical and biomechanical alterations induced by aneurysm dilatation in patientâ€specific ascending thoracic aortas. International Journal for Numerical Methods in Biomedical Engineering, 2020, 36, e3326.	1.0	9
43	Future directions for personalized computer simulations in endovascular aneurysms repair. International Journal of Cardiology, 2020, 304, 152-153.	0.8	Ο
44	A Chemomechanobiological Model of the Long-Term Healing Response of Arterial Tissue to a Clamping Injury. Frontiers in Bioengineering and Biotechnology, 2020, 8, 589889.	2.0	2
45	Mechanics-driven mechanobiological mechanisms of arterial tortuosity. Science Advances, 2020, 6, .	4.7	24
46	Structural Intensity Assessment on Shells via the Projection of Experimental Data on a Finite-Element Mesh. Conference Proceedings of the Society for Experimental Mechanics, 2020, , 53-58.	0.3	0
47	A Fast Method of Virtual Stent Graft Deployment for Computer Assisted EVAR. , 2020, , 147-169.		1
48	Local Stiffness Estimation of the Human Eardrum via the Virtual Fields Method. Lecture Notes in Computational Vision and Biomechanics, 2020, , 248-255.	0.5	0
49	Inverse identification of local stiffness across ascending thoracic aortic aneurysms. Biomechanics and Modeling in Mechanobiology, 2019, 18, 137-153.	1.4	39
50	On improving the accuracy of nonhomogeneous shear modulus identification in incompressible elasticity using the virtual fields method. International Journal of Solids and Structures, 2019, 178-179, 136-144.	1.3	18
51	Review of the Essential Roles of SMCs in ATAA Biomechanics. , 2019, , 95-114.		3
52	Identifying Local Arterial Stiffness to Assess the Risk of Rupture of Ascending Thoracic Aortic Aneurysms. Annals of Biomedical Engineering, 2019, 47, 1038-1050.	1.3	22
53	Structural intensity assessment on shells via a finite element approximation. Journal of the Acoustical Society of America, 2019, 145, 312-326.	0.5	6
54	Predictive Numerical Simulations of Double Branch Stent-Graft Deployment in an Aortic Arch Aneurysm. Annals of Biomedical Engineering, 2019, 47, 1051-1062.	1.3	30

#	Article	IF	CITATIONS
55	Patient-specific predictions of aneurysm growth and remodeling in the ascending thoracic aorta using the homogenized constrained mixture model. Biomechanics and Modeling in Mechanobiology, 2019, 18, 1895-1913.	1.4	51
56	Gradient-enhanced continuum models of healing in damaged soft tissues. Biomechanics and Modeling in Mechanobiology, 2019, 18, 1443-1460.	1.4	14
57	Constrained mixture modeling affects material parameter identification from planar biaxial tests. Journal of the Mechanical Behavior of Biomedical Materials, 2019, 95, 124-135.	1.5	20
58	Multiscale Mechanical Behavior of Large Arteries. , 2019, , 180-202.		1
59	Local variations in material and structural properties characterize murine thoracic aortic aneurysm mechanics. Biomechanics and Modeling in Mechanobiology, 2019, 18, 203-218.	1.4	52
60	Model reduction methodology for computational simulations of endovascular repair. Computer Methods in Biomechanics and Biomedical Engineering, 2018, 21, 139-148.	0.9	14
61	A non-invasive methodology for ATAA rupture risk estimation. Journal of Biomechanics, 2018, 66, 119-126.	0.9	17
62	Kinematics of collagen fibers in carotid arteries under tension-inflation loading. Journal of the Mechanical Behavior of Biomedical Materials, 2018, 77, 718-726.	1.5	36
63	Nonâ€affine fiber kinematics in arterial mechanics: a continuum micromechanical investigation. ZAMM Zeitschrift Fur Angewandte Mathematik Und Mechanik, 2018, 98, 2101-2121.	0.9	26
64	Evaluation of Peak Wall Stress in an Ascending Thoracic Aortic Aneurysm Using FSI Simulations: Effects of Aortic Stiffness and Peripheral Resistance. Cardiovascular Engineering and Technology, 2018, 9, 707-722.	0.7	54
65	Ascending thoracic aorta aneurysm repair induces positive hemodynamic outcomes in a patient with unchanged bicuspid aortic valve. Journal of Biomechanics, 2018, 81, 145-148.	0.9	17
66	Three-Dimensional Full-Field Strain Measurements across a Whole Porcine Aorta Subjected to Tensile Loading Using Optical Coherence Tomography–Digital Volume Correlation. Frontiers in Mechanical Engineering, 2018, 4, .	0.8	24
67	Numerical simulation of arterial remodeling in pulmonary autografts. ZAMM Zeitschrift Fur Angewandte Mathematik Und Mechanik, 2018, 98, 2239-2257.	0.9	22
68	Computational predictions of damage propagation preceding dissection of ascending thoracic aortic aneurysms. International Journal for Numerical Methods in Biomedical Engineering, 2018, 34, e2944.	1.0	20
69	A comprehensive study of layer-specific morphological changes in the microstructure of carotid arteries under uniaxial load. Acta Biomaterialia, 2017, 57, 342-351.	4.1	66
70	Patient-specific stress analyses in the ascending thoracic aorta using a finite-element implementation of the constrained mixture theory. Biomechanics and Modeling in Mechanobiology, 2017, 16, 1765-1777.	1.4	36
71	Fluid- and Biomechanical Analysis of Ascending Thoracic Aorta Aneurysm with Concomitant Aortic Insufficiency. Annals of Biomedical Engineering, 2017, 45, 2921-2932.	1.3	42
72	Importance of material parameters and strain energy function on the wall stresses in the left ventricle. Computer Methods in Biomechanics and Biomedical Engineering, 2017, 20, 1223-1232.	0.9	5

#	Article	IF	CITATIONS
73	Hyperelasticity of Soft Tissues and Related Inverse Problems. CISM International Centre for Mechanical Sciences, Courses and Lectures, 2017, , 37-66.	0.3	8
74	Subject-Specific Computational Prediction of the Effects of Elastic Compression in the Calf. , 2017, , 523-544.		1
75	Characteristics of thoracic aortic aneurysm rupture in vitro. Acta Biomaterialia, 2016, 42, 286-295.	4.1	24
76	Novel Methodology for Characterizing Regional Variations in the Material Properties of Murine Aortas. Journal of Biomechanical Engineering, 2016, 138, .	0.6	77
77	Local mechanical properties of human ascending thoracic aneurysms. Journal of the Mechanical Behavior of Biomedical Materials, 2016, 61, 235-249.	1.5	44
78	<i>In vivo</i> Identification of the Passive Mechanical Properties of Deep Soft Tissues in the Human Leg. Strain, 2016, 52, 400-411.	1.4	19
79	â€~Advances in Experimental Mechanics for Biomedical Soft Tissues and Materials'. Strain, 2016, 52, 371-371.	1.4	1
80	Biaxial rupture properties of ascending thoracic aortic aneurysms. Acta Biomaterialia, 2016, 42, 273-285.	4.1	105
81	Patient-specific simulation of endovascular repair surgery with tortuous aneurysms requiring flexible stent-grafts. Journal of the Mechanical Behavior of Biomedical Materials, 2016, 63, 86-99.	1.5	53
82	Predictive Models with Patient Specific Material Properties for the Biomechanical Behavior of Ascending Thoracic Aneurysms. Annals of Biomedical Engineering, 2016, 44, 84-98.	1.3	24
83	The fiber reorientation problem revisited in the context of Eshelbian micromechanics: theory and computations. Proceedings in Applied Mathematics and Mechanics, 2015, 15, 39-42.	0.2	4
84	Prediction of the Biomechanical Effects of Compression Therapy by Finite Element Modeling and Ultrasound Elastography. IEEE Transactions on Biomedical Engineering, 2015, 62, 1011-1019.	2.5	18
85	Patient specific stress and rupture analysis of ascending thoracic aneurysms. Journal of Biomechanics, 2015, 48, 1836-1843.	0.9	55
86	Prediction of the Biomechanical Effects of Compression Therapy on Deep Veins Using Finite Element Modelling. Annals of Biomedical Engineering, 2015, 43, 314-324.	1.3	25
87	Pointwise characterization of the elastic properties of planar soft tissues: application to ascending thoracic aneurysms. Biomechanics and Modeling in Mechanobiology, 2015, 14, 967-978.	1.4	34
88	Characterisation of Knee Brace Migration and Associated Skin Deformation During Flexion by Full-Field Measurements. Experimental Mechanics, 2015, 55, 349-360.	1.1	12
89	Evaluation of the mechanical efficiency of knee braces based on computational modeling. Computer Methods in Biomechanics and Biomedical Engineering, 2015, 18, 646-661.	0.9	7
90	Characterisation of in-vivo mechanical action of knee braces regarding their anti-drawer effect. Knee, 2015, 22, 80-87.	0.8	12

#	Article	IF	CITATIONS
91	Inverse problems in the mechanical characterization of elastic arteries. MRS Bulletin, 2015, 40, 317-323.	1.7	7
92	Patient-specific numerical simulation of stent-graft deployment: Validation on three clinical cases. Journal of Biomechanics, 2015, 48, 1868-1875.	0.9	80
93	The concept of frozen elastic energy as a consequence of changes in microstructure morphology. Computer Methods in Biomechanics and Biomedical Engineering, 2015, 18, 1966-1967.	0.9	2
94	Regional identification of mechanical properties in arteries. Computer Methods in Biomechanics and Biomedical Engineering, 2015, 18, 1874-1875.	0.9	4
95	Mechanical characterization of aortic valve tissues using an inverse analysis approach. Computer Methods in Biomechanics and Biomedical Engineering, 2015, 18, 1976-1977.	0.9	1
96	Material model calibration from planar tension tests on porcine linea alba. Journal of the Mechanical Behavior of Biomedical Materials, 2015, 43, 26-34.	1.5	8
97	Deployment of stent grafts in curved aneurysmal arteries: toward a predictive numerical tool. International Journal for Numerical Methods in Biomedical Engineering, 2015, 31, e02698.	1.0	43
98	Evaluation of the mechanical efficiency of knee orthoses: A combined experimental–numerical approach. Proceedings of the Institution of Mechanical Engineers, Part H: Journal of Engineering in Medicine, 2014, 228, 533-546.	1.0	3
99	Mechanical action of the blood onto atheromatous plaques: influence of the stenosis shape and morphology. Computer Methods in Biomechanics and Biomedical Engineering, 2014, 17, 527-538.	0.9	9
100	MRI strain imaging of the carotid artery: Present limitations and future challenges. Journal of Biomechanics, 2014, 47, 824-833.	0.9	18
101	In vitro analysis of localized aneurysm rupture. Journal of Biomechanics, 2014, 47, 607-616.	0.9	83
102	Numerical simulation of arterial dissection during balloon angioplasty of atherosclerotic coronary arteries. Journal of Biomechanics, 2014, 47, 878-889.	0.9	29
103	Comparing the Passive Biomechanics of Tension-Pressure Loading of Porcine Renal Artery and Its First Branch. Conference Proceedings of the Society for Experimental Mechanics, 2014, , 35-40.	0.3	0
104	Biomechanical response of varicose veins to elastic compression: A numerical study. Journal of Biomechanics, 2013, 46, 599-603.	0.9	27
105	Finite Element simulation of buckling-induced vein tortuosity and influence of the wall constitutive properties. Journal of the Mechanical Behavior of Biomedical Materials, 2013, 26, 119-126.	1.5	18
106	A New Method for the In Vivo Identification of Mechanical Properties in Arteries From Cine MRI Images: Theoretical Framework and Validation. IEEE Transactions on Medical Imaging, 2013, 32, 1448-1461.	5.4	12
107	Identification of the in vivo elastic properties of common carotid arteries from MRI: A study on subjects with and without atherosclerosis. Journal of the Mechanical Behavior of Biomedical Materials, 2013, 27, 184-203.	1.5	15
108	Assessment of the in-plane biomechanical properties of human skin using a finite element model updating approach combined with an optical full-field measurement on a new tensile device. Journal of the Mechanical Behavior of Biomedical Materials, 2013, 27, 273-282.	1.5	33

#	Article	IF	CITATIONS
109	Inverse problems and material identification in tissue biomechanics. Journal of the Mechanical Behavior of Biomedical Materials, 2013, 27, 129-131.	1.5	6
110	Biomechanics of Porcine Renal Arteries and Role of Axial Stretch. Journal of Biomechanical Engineering, 2013, 135, 81007.	0.6	21
111	Finite Element Analysis of the Mechanical Performances of 8 Marketed Aortic Stent-Grafts. Journal of Endovascular Therapy, 2013, 20, 523-535.	0.8	80
112	Patient-specific modelling of the calf muscle under elastic compression using magnetic resonance imaging and ultrasound elastography. Computer Methods in Biomechanics and Biomedical Engineering, 2013, 16, 332-333.	0.9	3
113	Patient-Specific Simulation of Devices-Tissues Interactions for Endovascular Aneurysm Repair. , 2013, , .		0
114	Patient-Specific Computational Models: Tools for Improving the Efficiency of Medical Compression Stockings. , 2013, , 25-37.		3
115	Editorial: Identification of material parameters through inverse finite element modelling. Computer Methods in Biomechanics and Biomedical Engineering, 2012, 15, 1-2.	0.9	6
116	Identification of the material parameters of soft tissues in the compressed leg. Computer Methods in Biomechanics and Biomedical Engineering, 2012, 15, 3-11.	0.9	45
117	Severe Bending of Two Aortic Stent-Grafts: An Experimental and Numerical Mechanical Analysis. Annals of Biomedical Engineering, 2012, 40, 2674-2686.	1.3	33
118	Mechanical identification of layer-specific properties of mouse carotid arteries using 3D-DIC and a hyperelastic anisotropic constitutive model. Computer Methods in Biomechanics and Biomedical Engineering, 2012, 15, 37-48.	0.9	37
119	Identification of heterogeneous elastic properties in stenosed arteries: a numerical plane strain study. Computer Methods in Biomechanics and Biomedical Engineering, 2012, 15, 49-58.	0.9	16
120	3D Residual Stress Field in Arteries: Novel Inverse Method Based on Optical Fullâ€field Measurements. Strain, 2012, 48, 528-538.	1.4	22
121	A numerical parametric study of the mechanical action of pulsatile blood flow onto axisymmetric stenosed arteries. Medical Engineering and Physics, 2012, 34, 1483-1495.	0.8	22
122	Efficiency of Knee Braces: A Biomechanical Approach Based on Computational Modeling. , 2012, , .		1
123	Experimental characterization of rupture in human aortic aneurysms using a full-field measurement technique. Biomechanics and Modeling in Mechanobiology, 2012, 11, 841-853.	1.4	67
124	Computational comparison of the bending behavior of aortic stent-grafts. Journal of the Mechanical Behavior of Biomedical Materials, 2012, 5, 272-282.	1.5	79
125	Patient-Specific Modeling of Leg Compression in the Treatment of Venous Deficiency. Studies in Mechanobiology, Tissue Engineering and Biomaterials, 2011, , 217-238.	0.7	3
126	In vivo velocity vector imaging and time-resolved strain rate measurements in the wall of blood vessels using MRI. Journal of Biomechanics, 2011, 44, 979-983.	0.9	7

#	Article	IF	CITATIONS
127	Characterisation of failure in human aortic tissue using digital image correlation. Computer Methods in Biomechanics and Biomedical Engineering, 2011, 14, 73-74.	0.9	5
128	In Vitro Characterisation of Physiological and Maximum Elastic Modulus of Ascending Thoracic Aortic Aneurysms Using Uniaxial Tensile Testing. European Journal of Vascular and Endovascular Surgery, 2010, 39, 700-707.	0.8	128
129	Anisotropic and hyperelastic identification of in vitro human arteries from full-field optical measurements. Journal of Biomechanics, 2010, 43, 2978-2985.	0.9	126
130	Extension of the virtual fields method to elasto-plastic material identification with cyclic loads and kinematic hardening. International Journal of Solids and Structures, 2010, 47, 2993-3010.	1.3	71
131	Inverse methods for characterizing the anisotropic hyperelastic behaviour of arteries in vitro. EPJ Web of Conferences, 2010, 6, 18001.	0.1	0
132	Comparison of two approaches for differentiating full-field data in solid mechanics. Measurement Science and Technology, 2010, 21, 015703.	1.4	46
133	Mixed Experimental and Numerical Approach for Characterizing the Biomechanical Response of the Human Leg Under Elastic Compression. Journal of Biomechanical Engineering, 2010, 132, 031006.	0.6	42
134	In vivo measurements of blood viscosity and wall stiffness in the carotid using PC-MRI. European Journal of Computational Mechanics, 2009, 18, 9-20.	0.6	8
135	Variation of transverse and shear stiffness properties of wood in a tree. Composites Part A: Applied Science and Manufacturing, 2009, 40, 1953-1960.	3.8	43
136	Local stiffness reduction in impacted composite plates from full-field measurements. Composites Part A: Applied Science and Manufacturing, 2009, 40, 1961-1974.	3.8	27
137	Étude mécanique des articles de contention et de leurs effets sur la jambe humaine. Mecanique Et Industries, 2009, 10, 7-13.	0.2	0
138	Stress Reconstruction and Constitutive Parameter Identification in Plane-Stress Elasto-plastic Problems Using Surface Measurements of Deformation Fields. Experimental Mechanics, 2008, 48, 403-419.	1.1	73
139	3D Heterogeneous Stiffness Reconstruction Using MRI and the Virtual Fields Method. Experimental Mechanics, 2008, 48, 479-494.	1.1	48
140	Identification of Heterogeneous Constitutive Parameters in a Welded Specimen: Uniform Stress and Virtual Fields Methods for Material Property Estimation. Experimental Mechanics, 2008, 48, 451-464.	1.1	70
141	Overview of Identification Methods of Mechanical Parameters Based on Full-field Measurements. Experimental Mechanics, 2008, 48, 381-402.	1.1	594
142	Identification of elasto-visco-plastic parameters and characterization of Lüders behavior using digital image correlation and the virtual fields method. Mechanics of Materials, 2008, 40, 729-742.	1.7	119
143	Characterization of composite plates using the virtual fields method with optimized loading conditions. Composite Structures, 2008, 85, 70-82.	3.1	27
144	Estimation of the strain field from full-field displacement noisy data. European Journal of Computational Mechanics, 2008, 17, 857-868.	0.6	51

9

#	Article	IF	CITATIONS
145	Viscoelastic material properties' identification using full field measurements on vibrating plates. , 2008, , .		1
146	Software Implementation of the Virtual Fields Method. Applied Mechanics and Materials, 2007, 7-8, 57-62.	0.2	0
147	Novel experimental approach for longitudinal-radial stiffness characterisation of clear wood by a single test. Holzforschung, 2007, 61, 573-581.	0.9	56
148	General framework for the identification of constitutive parameters from full-field measurements in linear elasticity. International Journal of Solids and Structures, 2007, 44, 4978-5002.	1.3	130
149	Identification of the Orthotropic Elastic Stiffnesses of Composites with the Virtual Fields Method: Sensitivity Study and Experimental Validation. Strain, 2007, 43, 250-259.	1.4	81
150	Identification of 3-D Heterogeneous Modulus Distribution With the Virtual Fields Method. , 2007, , 663-664.		0
151	Experimental identification of a nonlinear model for composites using the grid technique coupled to the virtual fields method. Composites Part A: Applied Science and Manufacturing, 2006, 37, 315-325.	3.8	65
152	Identification of the through-thickness rigidities of a thick laminated composite tube. Composites Part A: Applied Science and Manufacturing, 2006, 37, 326-336.	3.8	41
153	Identification of Elasto-Plastic Constitutive Parameters from Statically Undetermined Tests Using the Virtual Fields Method. Experimental Mechanics, 2006, 46, 735-755.	1.1	66
154	Optimization of the Unnotched Iosipescu Test on Composites for Identification from Full-Field Measurements. Applied Mechanics and Materials, 2006, 5-6, 125-134.	0.2	2
155	The Virtual Fields Method for Extracting Constitutive Parameters From Full-Field Measurements: a Review. Strain, 2006, 42, 233-253.	1.4	180
156	The Virtual Fields Method for Extracting Constitutive Parameters From Fullâ€Field Measurements: a Review. Strain, 2006, 42, 233-253.	1.4	34
157	A multi-scale approach for crack width prediction in reinforced-concrete beams repaired with composites. Composites Science and Technology, 2005, 65, 445-453.	3.8	6
158	Characterization of the Nonlinear Shear Behaviour of UD Composite Materials Using the Virtual Fields Method. Applied Mechanics and Materials, 2005, 3-4, 185-190.	0.2	1
159	Identification of the Through-Thickness Orthotropic Stiffness of Composite Tubes from Full-Field Measurements. Applied Mechanics and Materials, 2005, 3-4, 161-166.	0.2	1
160	Sensitivity of the virtual fields method to noisy data. Computational Mechanics, 2004, 34, 439-452.	2.2	156
161	Grid method: Application to the characterization of cracks. Experimental Mechanics, 2004, 44, 37-43.	1.1	35
162	A full-field optical method for the experimental analysis of reinforced concrete beams repaired with composites. Composites Part A: Applied Science and Manufacturing, 2004, 35, 873-884.	3.8	34

#	Article	IF	CITATIONS
163	Mechanical behavior of RC beams reinforced by externally bonded CFRP sheets. Materials and Structures/Materiaux Et Constructions, 2003, 36, 522-529.	1.3	17
164	Mechanical behavior of cracked beams strengthened with composites: application of a full-field measurement method. Materials and Structures/Materiaux Et Constructions, 2003, 36, 379-385.	1.3	3
165	Mechanical behavior of RC beams reinforced by externally bonded CFRP sheets. Materials and Structures/Materiaux Et Constructions, 2003, 36, 522-529.	1.3	6
166	Evaluation of image registration for measuring deformation fields in soft tissue mechanics. Strain, 0,	1.4	0